Journal of The Electrochemical Society, **148** (10) C663-C667 (2001)
0013-4651/2001/148(10)/C663/5/$7.00 © The Electrochemical Society, Inc.

Electrochemical Impedance Spectroscopy of 6H-SiC in Aqueous Hydrofluoric Acid

Jonathan E. Spanier,[a,*,c] Alan C. West,[b,] and Irving P. Herman[a,z]**

[a]*Department of Applied Physics and Applied Mathematics and* [b]*Department of Chemical Engineering and the Materials Research Science and Engineering Center, Columbia University, New York, New York 10027, USA*

Polarization and electrochemical impedance spectroscopy of p-type 6H-SiC electrodes in an aqueous hydrofluoric acid solution is performed during the formation of porous SiC. The polarization of p-type SiC permits the identification of the flatband voltage, a Tafel-like region, and a limiting current which is attributed to the onset of the electropolishing regime. For some of the potential range studied over which porous layers form, the impedance data are characterized by a single high-frequency semicircle and there is a second low-frequency semicircle at intermediate potentials. The dependence of the fitted capacitance and resistance on the applied voltage suggests that the SiC-electrolyte interface is controlled under different regimes of potential by the space-charge layer, the interaction with surface states, and the formation of a passivating film.
 [DOI: 10.1149/1.1396652]

Manuscript submitted November 1, 2000; revised manuscript received May 15, 2001. Available electronically August 24, 2001.

The formation of porous silicon carbide (PSC) has been observed under the anodic bias of both n-type and p-type SiC in aqueous hydrofluoric acid solutions.[1,2] Since SiC has no known wet etchants, the electrochemical and photoelectrochemical etching of SiC remains the only practical and efficient means of etching in applications that demand significantly higher etch rates than those offered by reactive ion etching and plasma etching. Further, electrochemical and photoelectrochemical etching of SiC is the only basis for dopant selectivity in SiC etching.[3] PSC has been of interest recently because it exhibits a visible room-temperature photoluminescence[4] and as such has been used in electroluminescent devices.[5] It has also been used as a material for power device passivation[6] and hydrocarbon gas sensors,[7] and as a substrate for high-quality regrowth.[8] PSC is also more stable than porous silicon with regard to oxidation at room temperature.[9]

Electrochemical studies provide necessary information about the anodization process and also some insight into the fundamentals of the charge-transfer and dissolution processes. Polarization measurements can provide information about the range of potentials and current densities over which current flows and an anodic film evolves and/or dissolution takes place. The time-dependent nature of these polarizations can potentially provide information about how an evolving porous layer may affect charge transfer at the semiconductor-electrolyte interface. The sensitivity of a polarization response to the sweep rate and the hysteretic behavior may suggest a time scale over which a passivating film may be formed and dissolved, or adsorbed and desorbed. Since electrochemical impedance spectroscopy (EIS) is carried out over a range of frequencies, it often provides more information about charge transfer at the interface than polarization measurements alone. When a kinetic model of the charge transfer appropriate for the system is paired with the measured response, kinetic parameters can be determined. Such has been the approach of Vanmaekelburgh and Searson[10] in examining the silicon-HF interface at different overpotentials. Others have used EIS in conjunction with other experimental techniques to study the silicon-aqueous HF interface during the formation of porous silicon.[11-13]

Further, the time evolution of a nano- or microporous layer during the anodization of silicon and silicon carbide and the resulting structural gradients of porosity and crystallite size across the thickness of the porous layer raise questions about the time dependence of the semiconductor-electrolyte interface characteristics and kinetic parameters. The time dependence of the impedance response can offer new clues into the charge transfer through the evolving porous semiconductor electrodes. In the case of SiC, Lauermann *et al.*[14] identified unstable, time-dependent behavior of the interfacial capacitance of 6H-SiC in both alkaline and acidic solutions under anodic bias. The authors were evidently aware that a corroded layer forms on the surface of the SiC anode, but failed to identify its crystalline nature and did not investigate the nature of the time dependence of the interfacial capacitance. van de Lagemaat *et al.*[15] have carried out photoelectrochemical impedance spectroscopy of n-type 6H-SiC in aqueous H_2SO_4 solutions.

The present work demonstrates that electrochemical impedance spectroscopy of SiC during electrochemical anodic dissolution permits the identification and study of layers that affect charge transfer. It is seen that the formed porous layer does not significantly impede charge transfer.

Experimental

6H-SiC substrates of the p-type ($N_A \approx 10^{18}\,cm^{-3}$) were metallized with 1000 and 4000 Å thick films of sputtered Ti and Pt. The metallization was annealed in N_2 at 1000°C for 30 s to produce ohmic contacts. Leads were attached and the samples encapsulated in Apezion wax, exposing a small area (~0.5 cm^2) of the polished $(000\bar{1})$ face. The samples were immersed in an aqueous and ethanolic hydrofluoric acid solution, and anodically biased in the dark. A peristaltic pump was used to free bubbles which evolved on the semiconductor electrode during the anodic dissolution and to ensure that the solution was well-mixed, and flow was directed across the surface of the electrode.

It is generally understood that in the electropolishing regime in silicon (the potential range above which porous Si forms) the current is particularly sensitive to mass transport effects. Hysteresis in cyclic voltammograms has been shown to be minimized using rotating disk electrodes[16] and therefore steady-state investigations of silicon electropolishing are best performed under uniformly accessible hydrodynamic electrodes.[17] Our discussion focuses primarily on the region of porous layer formation in SiC, and studies of the dependence of the polarization and impedance response on flow conditions were not performed.

The SiC-aqueous HF interface was analyzed by polarization and EIS. The impedance measurements were conducted at different current densities and at different stages of anodic dissolution. The data acquisition was carried out using an EG&G potentiogalvanostat and a Solartron 1255 frequency response analyzer interfaced to a PC equipped with Z-Plot 2.0 software. The impedance was measured at selected frequencies over the range 0.1 Hz to 100 kHz. While PSC is normally prepared galvanostatically, the impedance data were taken under potential control, and all potentials were referenced to the

* Electrochemical Society Student Member.
** Electrochemical Society Active Member.
[c] Present address: Department of Chemistry and Chemical Biology, Harvard University, Cambridge, MA 02138, USA.
[z] E-mail: iph1@columbia.edu

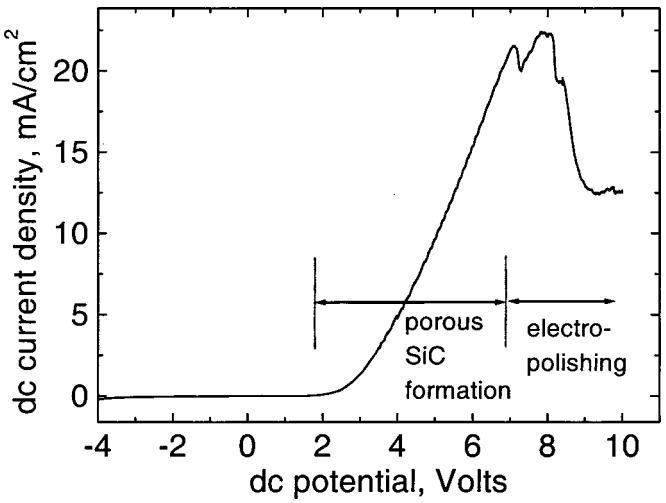

Figure 1. Polarization of p-type 6H-SiC electrode in 2.5% aqueous hydrofluoric acid. The potential is referenced to the counter electrode.

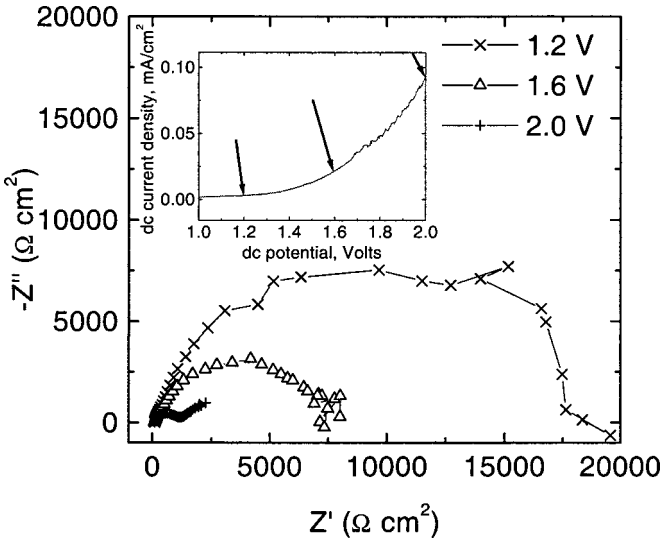

Figure 2. AC impedance response for $1.2 < V < 2.0$. Frequency is an implicit variable that starts at 100 kHz near $Z' = Z'' = 0$ and monotonically decreases along the curve to 0.1 Hz. The inset shows the corresponding potentials, with the arrows pointing to the potentials studied. The potential is referenced to the counter electrode.

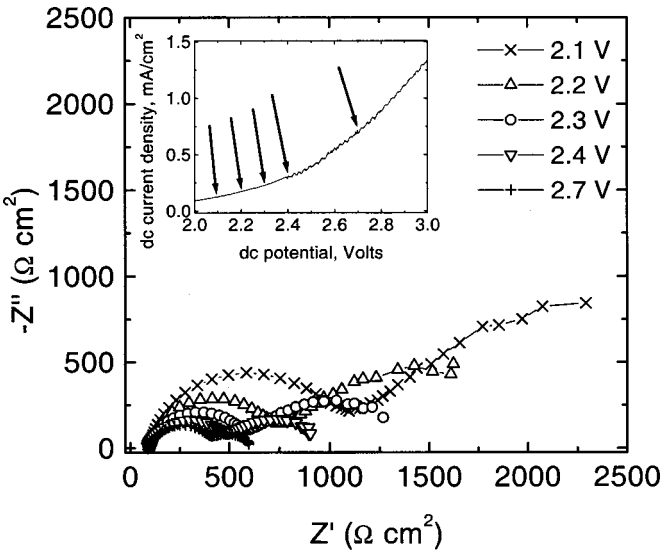

Figure 3. AC impedance response for $2.1 < V < 2.7$.

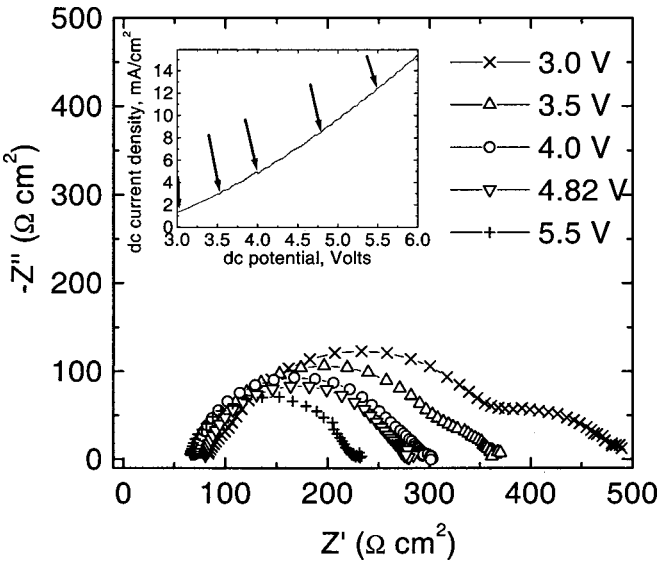

Figure 4. AC impedance response for $3.0 < V < 5.5$.

counter electrode (a Pt wire), V_{ce}. The impedance response was unstable during the initial polarization of the electrode and settled to a stable and reproducible response within 1 min of polarizing the electrode. The selected peak-to-peak value of the ac potential was always less than 3% of the dc value and was chosen so that the response was linear; the applied ac voltages were selected in a random order.

Results

Polarization measurements.—Figure 1 shows the polarization of a p-type 6H-SiC electrode in a solution composed of 2.5 vol % HF (diluted from 49% HF, reagent grade), 48.5% deionized H_2O, and 48.5% C_2H_5OH, taken at a sweep rate of 100 mV/s within 1 min after the initial polarization of the electrode. The polarization of the n-type SiC electrode in the dark was unstable (not shown). The flatband voltage is approximately 2 V, and the current density peaks between 7 and 8 V. The flatband voltage is in reasonable agreement with published values referenced to a saturated calomel electrode (SCE),[14,18-20] and the polarization is consistent with the other published work for a similar concentration of HF.[20]

Impedance measurements.—Figure 2 shows the impedance response of the electrode at three different applied dc potentials (1.2, 1.6, and 2.0 V) which are denoted by arrows in the inset. The impedance responses over a range of selected potentials from 2.1 to 8 V are shown in Fig. 3, 4, and 5. The response at very low overpotentials is characterized by a single large semicircle and for moderate overpotentials it is characterized by two distinct semicircles. For higher overpotentials (>3.5 V) the lower frequency semicircle is no longer discerned and the response consists of one semicircle. The responses at the high-frequency limit (100 kHz) for different values of the applied potential were nearly identical.

In Fig. 6, the measured resistance (as determined by the difference between the real part of the impedance at the high-frequency limit and the real part of the impedance at the low-frequency limit) is plotted as a function of the reciprocal of the dc current over a range corresponding to overpotentials between 2.3 and 5.5 V. The data agree reasonably with a linear fit, indicating that the system is

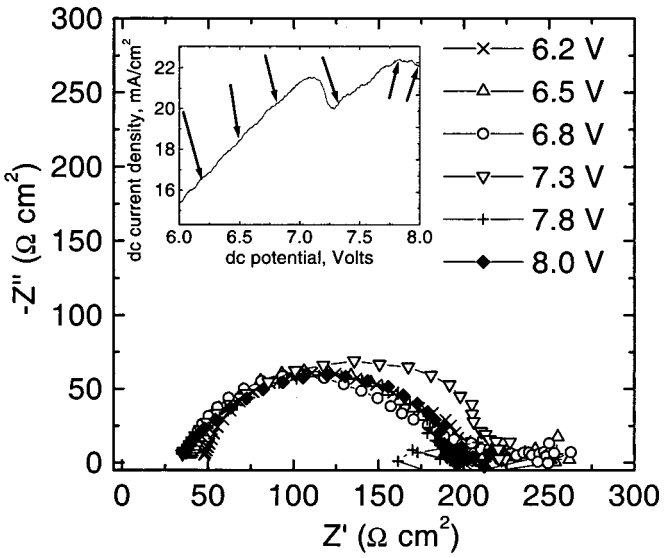

Figure 5. AC impedance response for $6.2 < V < 8.0$.

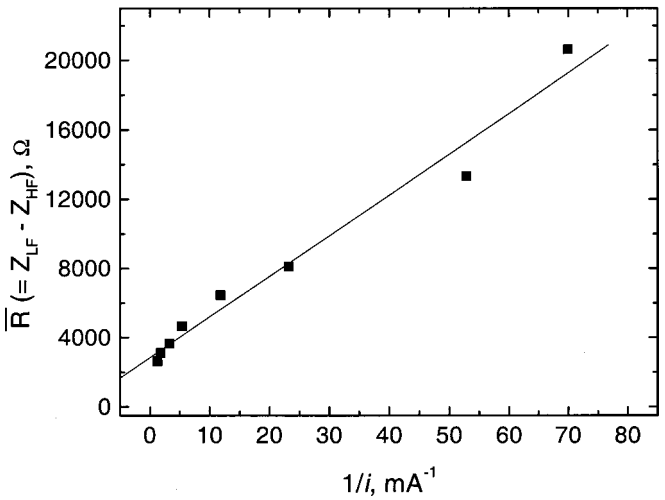

Figure 6. Difference between high- and low-frequency limit of impedance $\overline{R}$ as a function of inverse dc current, showing Tafel-like kinetics with linear regression-fitted slope of ~235 mV.

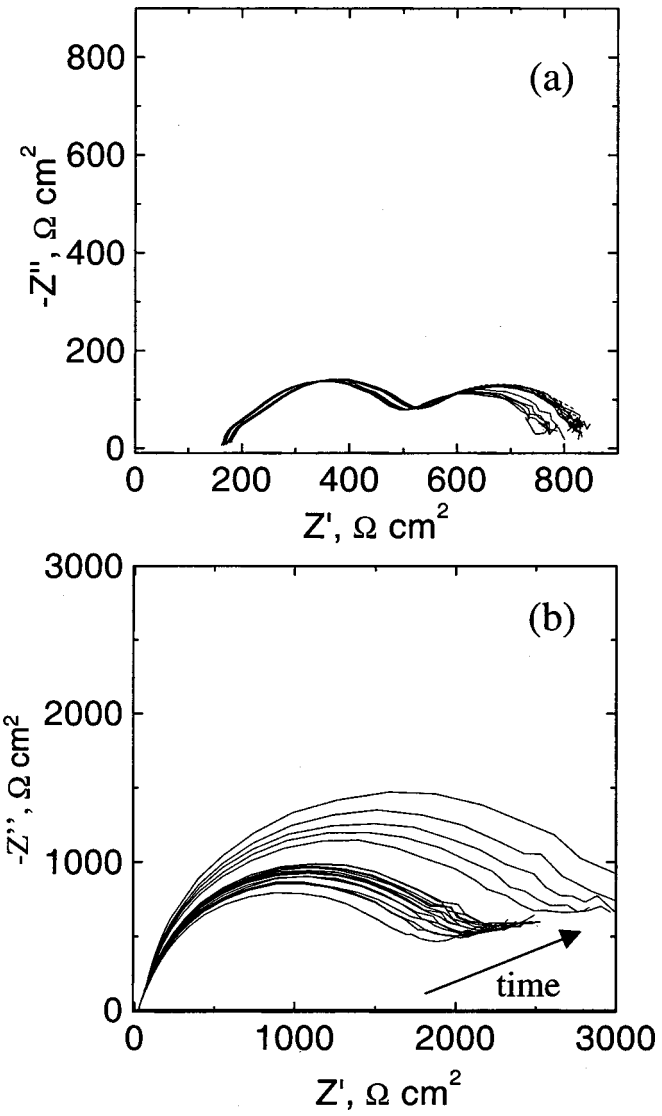

Figure 7. AC impedance response taken at different times during the course of a 90 min anodization at J = (a) 0.69 mA/cm^2, 2.7 V and (b) 0.05 mA/cm^2, 1.8 V.

Tafel-like, with a slope of ~235 mV. The apparent anodic transfer coefficient, from the Tafel slope, $2.303RT/\alpha_a F$ (F = 96,487 C/equiv), is determined to be $\alpha_a \simeq 0.25$. For comparison, in silicon in the region of pore formation, this effective transfer coefficient has been reported to be $\alpha_a = 1$, corresponding to a Tafel slope of 60 mV.[10,d]

The impedance response was also studied as a function of time for different applied potentials. Figure 7 shows the impedance response at a current density of (a) 0.69 and (b) 0.05 mA/cm^2 over the course of approximately 90 min. The response at moderate current density (a) is relatively stable, while that of (b) evolves toward larger and larger semicircular arcs. (The time intervals between successive sets of impedance measurements are not the same.)

[d] In fact, there is general agreement that at least in the potential range of porous Si formation, the dissolution is divalent. The apparent anodic transfer coefficient α_a is the product of the number of elementary charges transferred per mole ($n = 2$) and the anodic transfer coefficient ($\alpha = 0.5$). There is still some debate as to whether the dissolution occurs in one step (two holes captured at surface bonds) or two steps, in which a single hole capture is preceded by a second hole capture or an electron injection.

Discussion

The elementary reactions for the dissolution of silicon in aqueous HF solutions have been proposed and the model predictions of the impedance response based on these reactions agree reasonably with experiment;[10] the dissolution of SiC in aqueous HF is significantly more complicated. It is has been suggested that the dissolution of SiC involves the competition of oxidation of SiC and dissolution of the formed oxide according to[21]

$$SiC + 4H_2O + 8h^+ \rightarrow SiO_2 + CO_2\uparrow + 8H^+ \quad [1]$$

$$SiC + 2H_2O + 4h^+ \rightarrow SiO + CO\uparrow + 4H^+ \quad [2]$$

and the oxide formed from the first reaction is dissolved via[22]

$$SiO_2 + 6HF \rightarrow 2H^+ + SiF_6^{2-} + 2H_2O \quad [3]$$

SiO is also presumed to be dissolved in HF. Shor and Osgood[23] and Rysy *et al.*[20] have determined by coulometric means the average valency of the first two reactions to be slightly more than six elementary charges per mole, indicating that the first reaction occurs with a slightly higher probability than the second.

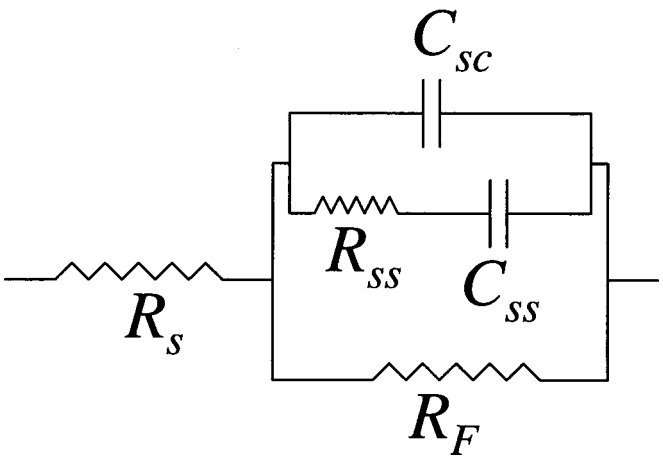

Figure 8. Equivalent circuit used to interpret the impedance response. R_s is the series resistance times area, R_F the faradaic resistance times area, C_{sc} the space-charge capacitance per unit area, and R_{ss} and C_{ss} the surface state resistance times area and capacitance per unit area, respectively.

The current is expected to be limited by the concentration of holes at the semiconductor surface, reactants (OH^- ions) at the interface (dependent upon HF concentration and flow), and the rate of charge transfer. It is known for other anodic semiconductor dissolution processes that the polarization response has two regimes: a range of lower potentials for which current is governed by the hole supply (kinetic control) and a range of higher potentials for which the current is under mass-transport control.[24] The supply of holes to the surface is

$$p_s = p_{bulk} \exp\left(\frac{eV_{sc}}{kT}\right) \quad [4]$$

where V_{sc} is the potential drop across the space-charge layer ($V_{sc} < 0$ for depletion, >0 for accumulation). (For applied potentials less than the flatband potential, the surface of the p-type electrode is in depletion of holes; for applied potentials larger than the flatband voltage, it is in accumulation.)

It is assumed that the first step in the dissolution process involves a hole capture at a surface bond. The rate of this step can be expressed as

$$v = kp_s x \quad [5]$$

where the rate constant k can be interpreted as being the product of the mean thermal velocity of a hole and the hole capture cross section, and x is the concentration of surface bonds. Lincot and Vedel[25] have shown that since this hole capture implies a transfer of charge across the Helmholtz layer, k must be of the form of the Butler-Volmer equation

$$k = k_0 \exp\left[\alpha\left(\frac{eV_H}{kT}\right)\right] \quad [6]$$

where α is the charge-transfer coefficient, k_0 a pre-exponential rate constant, and V_H the potential difference across the Helmholtz layer. Under the assumption that this first step is the rate-determining one, the current density is

$$j = envn \quad [7]$$

where n is the average valency. The current density is then

$$j = enk_0 x N_A \exp\left(\frac{eV_{sc}}{kT} + \frac{e\alpha V_H}{kT}\right) \quad [8]$$

where $p_{bulk} \equiv N_A$. For applied potential V and flatband potential V_{FB}, $V - V_{FB} = V_{sc} + V_H$. Our experimental observation is that

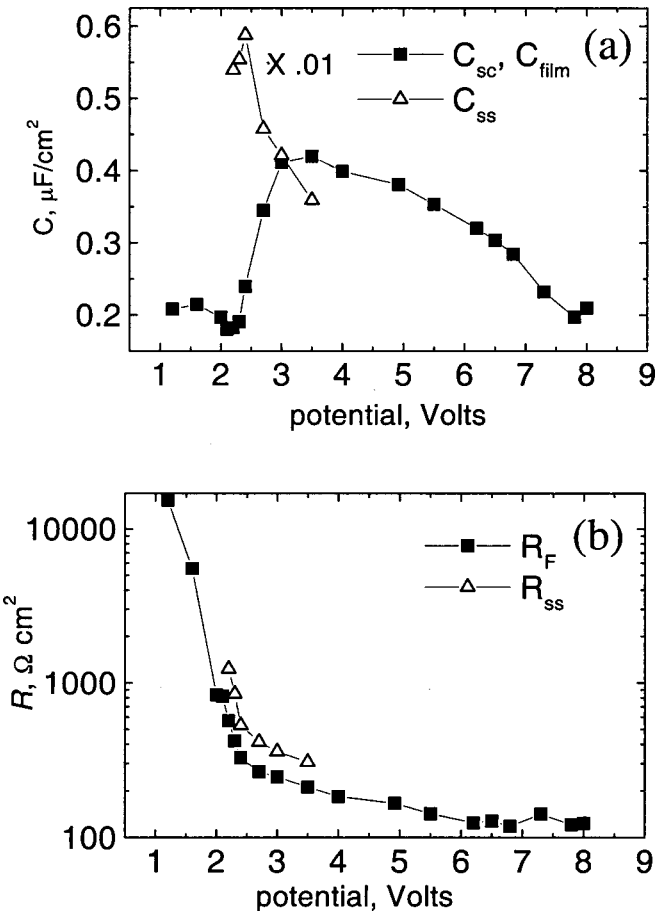

Figure 9. Fitted (a) capacitances per unit area and (b) resistances times area as a function of applied potential. C_{SS} has been multiplied by 0.01.

the slope $d(\log j)/dV$ is nearly linear in accord with Eq. 8 and is therefore Tafel-like. Without further information about the elementary kinetics, however, it is difficult to determine what Tafel slope should be expected for this system. Equation 8 is the result of a reasonable but highly simplified account of the polarization behavior in the potential region below electropolishing, and only serves to show that the current may depend on two potential drops: one across the space-charge layer and one across the Helmholtz layer; the polarization response in SiC is undoubtedly more complicated.

The impedance response in porous SiC appears to have three regimes: (1) potentials well below the flatband potential (1.2 and 1.6 V) for which the impedance is characterized by a single large loop as seen in Fig. 2, (2) potentials from 2.0 to approximately 4.0 V, for which two loops can be discerned as seen in Fig. 2-4, and (3) potentials above 4.0 V for which a single loop is observed as shown in Fig. 4 and 5. The response is qualitatively similar to that observed in p-type porous silicon by Ozanam *et al.*[26] These authors observed a single loop at potentials negative with respect to the flatband potential, a second, low-frequency loop at intermediate potentials along with an inductive loop, and at potentials above the regime of porous silicon formation, a high-frequency capacitive loop. The single loop at low potentials was attributed to the space-charge capacitance. The capacitive part the second, low-frequency loop was attributed to the existence of surface states and the inductive behavior to the enhancement of the specific surface area associated with the formation of the porous layer. The capacitance at high potentials was attributed to the formation of a thin oxide layer. A simple model of the role of surface states in charge transport and the impedance response at a silicon-electrolyte interface has been proposed by Oskam *et al.*[27]

For regimes (1) and (2) in SiC, the measured response is inter-

preted within the context of one of the equivalent circuits proposed in Ref. 26, as shown in Fig. 8. (For regime (3), the upper branch in Fig. 8 is replaced by a single capacitor C_{film}.) The fitted values of C and R are shown in Fig. 9a and b, respectively, as a function of applied voltage. The capacitance per unit area of the high-frequency loop (■) is observed to increase sharply from ~180 nF/cm^2 in the vicinity of the flatband voltage at the onset of appreciable current flow (between 2 and 3 V), peaking just above 400 nF/cm^2, and then decreases relatively slowly with increased potential. The capacitance per unit area C_{ss} of the low-frequency loop (△) is approximately 100 times larger, and decreases over the range of potential for which it can be observed.

In regime (1), the high-frequency capacitance C_{sc} is attributed to the space-charge layer and its magnitude is consistent with that expected for a SiC electrode of this doping concentration. The second, lower frequency loop in regime (2) is attributed to surface states (expected to be present in the energy gap of a semiconductor) having a collective capacitance per unit area C_{ss} (36–59 μF/cm^2) and resistance times area R_{ss}. The single loop in regime (3) is attributed to the formation of a passivating film (probably an oxide) and the decrease in the fitted capacitance per unit area C_{film} with increased potential is consistent with an increase in the film thickness. However, we do not wish to imply that a passivating film is only present in regime (3), but instead, that the film may simply not be detected by impedance spectroscopy in the other regimes. In contrast to porous silicon, an inductive, low-frequency loop is not observed in the potential range of porous SiC formation. It is not clear whether the inductive behavior is absent or the signal is too weak to be measured.

For potentials well below the flatband potential, the band bending at the interface prevents surface states from being occupied (or participating in charge transfer) and changes in the electrode potential are fully accounted for by the band bending across the space-charge layer; this corresponds to regime (1) for which the potential drop is solely across the space-charge layer. For more positive potentials very near and above the flatband potential [regime (2)], holes can be transferred from the valence band into surface states, giving rise to this second capacitance per unit area C_{ss}. In the limit of sufficiently high surface state concentration, the surface state capacitance is the Helmholtz capacitance. One possible interpretation is that in the limits of low and high potential, the high-frequency capacitance loop is due exclusively to the space-charge layer and the dielectric response of an oxide film, respectively, and a combination of these effects at intermediate potentials. The low-frequency capacitance at intermediate potentials is significantly larger in magnitude and is attributed to surface states. There are then three possibilities at each value of the applied potential for regimes (1) and (2): (a) the potential applied appears solely across the space-charge layer, (b) it is across the Helmholtz layer only, or (c) it is distributed across both. For example, in the anodic dissolution of p-type GaAs, some have interpreted the 60 mV Tafel slope to be evidence of space-charge layer control.[28,29] Others have provided evidence, based particularly on the low-frequency impedance response, that this dissolution proceeds under Helmholtz layer control.[30] The fitted value of C_{sc} near the flatband potential is in reasonable agreement with the expected value for an SiC electrode of this doping concentration; however, the values and dependence of the fitted resistance times area are not consistent with those generated by Eq. 8 for any reasonable values for k_0 and α.[e] Despite the reasonable values for C_{sc}, the Tafel-like slope of ~235 mV and the appearance of a low-frequency capacitance in regime (2) indicate that the system cannot be under space-charge layer control only, even within the range of porous layer formation.

[e] $k_0(=v_{th}\sigma)$ is estimated to be 10^{-14} cm^3/s, where v_{th} and σ are the thermal velocity and hole capture cross section, respectively. $v_{th} \approx 10^7$ cm/s and $\sigma \approx 10^{-21}$ cm^2 and $0.01 < \alpha < 2$.

Conclusions

The impedance response of a highly doped p-type SiC electrode in aqueous HF was measured for a range of potentials. The impedance response is characterized by a single, high-frequency semicircle for low potentials, an additional low-frequency semicircle for intermediate potentials, and a single semicircle at high potentials. The impedance response as a function of inverse current suggests that the charge transfer is Tafel-like. While the magnitude of the fitted capacitance is consistent with the expected value for the SiC electrode space-charge layer, the impedance response is likely due to a combination of the space-charge layer, the interaction of surface states, and the formation of a passivating film. Following the initial polarization of the electrode, the impedance response with time is highly stable for up to 90 min of anodization time, which indicates that the evolving porous layer does not significantly impede charge transfer.

Acknowledgments

This work is supported in part by the NSF Materials Research Science and Engineering Center under award no. DMR-9809687 and Kulite Semiconductor Products, Incorporated, in Leonia, NJ.

Columbia University assisted in meeting the publication costs of this article.

References

1. J. S. Shor, L. Bemis, A. D. Kurtz, I. Grimberg, B. Z. Weiss, M. F. MacMillan, and W. J. Choyke, *J. Appl. Phys.*, **76**, 4045 (1994).
2. J. S. Shor, I. Grimberg, B. Z. Weiss, and A. D. Kurtz, *Appl. Phys. Lett.*, **62**, 2836 (1993).
3. J. S. Shor, A. D. Kurtz, I. Grimberg, B. Z. Weiss, and R. M. Osgood, *J. Appl. Phys.*, **81**, 1546 (1997).
4. T. Matsumoto, J. Takahashi, T. Tamaki, T. Fugati, H. Mimura, and Y. Kanemitsu, *Appl. Phys. Lett.*, **64**, 226 (1994).
5. H. Mimura, T. Matsumoto, and Y. Kanemitsu, *Appl. Phys. Lett.*, **65**, 3350 (1994).
6. C. I. Harris, A. O. Konstantinov, C. Hallen, and E. Janzen, *Appl. Phys. Lett.*, **66**, 1501 (1995).
7. V. B. Shields, M. A. Ryan, R. M. Williams, M. G. Spencer, D. M. Collins, and D. Zhang, in *Silicon Carbide and Related Materials 1995*, S. Nakashima, H. Matsunami, S. Yoshida, and H. Harima, Editors, No. 142, Chap. 7, p. 1067, Institute of Physics, London (1966).
8. J. E. Spanier, G. T. Dunne, L. B. Rowland, and I. P. Herman, *Appl. Phys. Lett.*, **76**, 3879 (2000).
9. J. E. Spanier, G. S. Cargill III, I. P. Herman, S. Kim, D. R. Goldstein, A. D. Kurtz, and B. Z. Weiss, *Mater. Res. Soc. Symp. Proc.*, **452**, 491 (1997).
10. D. Vanmaekelbergh and P. C. Searson, *J. Electrochem. Soc.*, **141**, 697 (1994).
11. L. M. Peter, D. J. Riley, and R. I. Wielgosz, *Appl. Phys. Lett.*, **66**, 2355 (1995).
12. N. Koshida and K. Echizenya, *J. Electrochem. Soc.*, **138**, 837 (1991).
13. J. Ronga, A. Bsiesy, F. Gaspard, R. Hérino, M. Ligeon, F. Muller, and A. Halimaoui, *J. Electrochem. Soc.*, **138**, 1403 (1991).
14. I. Lauermann, R. Memming, and D. Meissner, *J. Electrochem. Soc.*, **144**, 73 (1997).
15. J. van de Lagemaat, D. Vanmaekelbergh, and J. J. Kelly, *J. Appl. Phys.*, **83**, 6089 (1998).
16. M. Etman, M. Neumann-Spallart, J. N. Chzalviel, and F. Ozanam, *J. Electroanal. Chem.*, **301**, 259 (1991).
17. R. G. Compton, A. C. Fisher, and G. P. Tyley, *J. Appl. Electrochem.*, **21**, 295 (1991).
18. T. Inoue and T. Yamese, *Chem. Lett.*, **7**, 869 (1985).
19. A. Mannivannan, A. Fujishima, and G. V. S. Rao, *Ber. Bunsen-Ges. Phys. Chem.*, **92**, 1522 (1988).
20. S. Rysy, H. Sadowski, and R. Helbig, *J. Solid State Electrochem.*, **3**, 437 (1999).
21. I. Lauermann, D. Meissner, R. Memming, R. Reineke, and B. Kastening, *Dechema Monogr.*, **124**, 617 (1991).
22. H. Gerischer, P. Allongue, and V. C. Kieling, *Ber. Bunsen-Ges. Phys. Chem.*, **97**, 753 (1993).
23. J. S. Shor and R. M. Osgood, *J. Electrochem. Soc.*, **140**, L123 (1993); J. S. Shor and A. D. Kurtz, *J. Electrochem. Soc.*, **141**, 778 (1994).
24. J. J. Kelly and D. Vanmaekelbergh, in *Semiconductor Micromachining*, Vol. 1, S. A. Campbell and H. J. Lewerz, Editors, pp. 35-91, John Wiley, New York (1998).
25. D. Lincot and J. Vedel, *J. Electroanal. Chem.*, **220**, 179 (1987).
26. F. Ozanam, J.-N. Chazalviel, A. Radi, and M. Etman, *J. Electrochem. Soc.*, **139**, 2491 (1992).
27. G. Oskam, P. M. Hoffman, and P. C. Searson, *Phys. Rev. Lett.*, **76**, 1521 (1996).
28. W. P. Goomes and H. H. Goossens, *Adv. Electrochem. Electrochem. Eng.*, **3**, 1 (1993).
29. S. Lingier, W. P. Gomes, and F. Cardon, *Ber. Bunsen-Ges. Phys. Chem.*, **93**, 2 (1989).
30. B. H. Erné and D. Vanmaekelbergh, *J. Electrochem. Soc.*, **144**, 3385 (1997).